Second United Nations International Conference on the Peaceful Uses of Atomic Energy

A/CONF.15/P/142
SWEDEN
2 June 1958

ORIGINAL: ENGLISH

Confidential until official release during Conference

THE SINTERING OF URANIUM DIOXIDE

by

Ulf Runfors,* Nils Schönberg** and Roland Kiessling*

ABSTRACT

Sintering of uranium dioxide has been studied as a function of powder characteristics, compacting parameters and sintering conditions such as temperature, time and sintering atmosphere. These studies are briefly described. The importance of the prehistory of the powder is shown, and a few methods used for characterizing the powder are reviewed. The influence of the different parameters mentioned on different properties of the sintered pellets, such as density, O/U ratio, differential shrinkage, crystal growth and the shape, size and distribution of pores is discussed.

*AB Atomenergi, Stockholm, Sweden

** Kohlswa Jernverks AB, Kolsva, Sweden

1. INTRODUCTION

The interest in Sweden for UO_2 fuel and D_2O moderated reactors is great. For this reason a sintering method for UO_2 has had to be developed (1, 2). The UO_2-powder available for sintering is taken from the production line ending in U-metal. The work described in this paper is concerned with the efforts to make as efficient use as possible of this powder without radically changing the existing production line. In several parts our investigations overlap work published by other authors (3, 4). The special character of the powder used, however, has given some interesting aspects on the sintering process. A production line for the sintering of UO_2 has also been built up and is described in a separate paper (5).

The sintering of UO_2 has been studied as a function of three main variables, namely the powder properties, the compacting variables and the sintering process.

2. POWDER PROPERTIES

2.1 Powder characteristics

The part of the production line that is of interest for the sintering starts with a homogenous precipitation process where an ammonium uranate is precipitated with urea. The uranate is calcined at about 275°C to so called UO_3 which finally is reduced in hydrogen at 700°C (6). Powder produced through homogenous precipitation consists of well rounded grains. These grains consist of agglomerates of sub-micron crystals which in turn are composed of sub-grains. Rough mean values of the size of these three categories are 40, 0,3 and 0,03 microns. The crystals of the agglomerates stick together very loosely. Most standard powder determination methods for characterizing the powder fail because they generally involve some operation causing a partial break down of the agglomerates.

The general properties of the powder are inherited through all the different steps from the first precipitation down to UO_2. A thorough control of the precipitation of the uranate is therefore very important. The inheritance of the distribution of agglomerates from ammonium uranate to UO_3 and UO_2 is shown in fig. 1. The agglomerate distribution has been determined through counting. The shape of the agglomerates is the same in all three powders (7, 10). An electron microscope study of the crystals of the three powders has shown rather flat crystals of about the same size. To draw any further conclusion is difficult because the temperature of the powder in the electron beam quickly exceeds the decomposition temperature of ammonium uranate in vacuum. In addition to some information on pressability of the powder, the agglomerate distribution curves have revealed one rather strange phenomenon. Powders are generally expected to sinter better the smaller the grain size. Four powders produced in laboratory scale (fig. 2) and a few from the production show decreasing sinterability with increasing content of small sized agglomerates. 37 microns have been chosen as the upper limit of the small agglomerates. A few earlier tests have namely shown that the sieve fraction below 37 microns sintered much more poorly than any other larger agglomerate fraction. This indicates that small agglomerates should consist of large

crystals and large agglomerates of small crystals. We have found that the excess oxygen content in a couple of powders increases with growing agglomerate size, which in turn indicates a larger specific surface and a smaller crystal size. However, this has not yet been confirmed by electron microscope or X-ray technics.

Considerable work has been devoted to finding one powder characteristic by which sinterability could be predicted:

Specific surface measurements by gas permeability has, because of the agglomerate structure of the powder, given discouraging results. A few determinations using the B. E. T. nitrogen adsorption method look promising.

These measurements can be compared with the electron microscope photos of four different powders mentioned above. A clear tendency can be observed in the shape of the crystals that can be correlated with the sintered density; namely, the better a powder sinters, the thinner the crystals and the more numerous the crystals with holes (fig. 3).

One simple way to get a rough idea of the sinterability is to measure the bulk density. Although the spread in values is large there is a trend showing that decreasing bulk density gives increasing sintered density (fig. 4).

X-ray line broadening shows a qualitative agreement between decreasing crystalite size and increasing sinterability. It has still not been possible, however, to use this technic for a more quantitative treatment.

In comparing the shrinkage of these powders one finds that the ratio shrinkage along the lengths over shrinkage along the diameter of a cylindrical compact increases with increasing sinterability (fig. 5). This phenomenon can be explained by assuming that, in compacting, the flat crystals get oriented perpendicularly to the pressing direction. This tendency is stronger the thinner the crystal plates are. Since sintering can be regarded as removal of voids, it is easy to realize that the number of voids which must be removed per unit length is different in the pressing direction as compared to the perpendicular direction.

2.2 Powder process variables

The main process variables that influences sinterability are precipitation, calcining and reduction parameters. All three have been investigated.

The precipitation experiments have not yet been evaluated by pressing and sintering.

The calcining has been carried out in a rotating furnace. The parameters have been varied between 70°C and 800°C at a constant time of 20 minutes.

These products have afterwards been reduced at temperatures between 600 and 1000°C for 2 hours. Evaluation of the results has been made by pressing at constant specific pressure and sintering under constant conditions. The results are shown in fig. 6. In order to reduce the errors caused by

pressing at constant pressure to different densities the difference between the sintered and pressed density has been plotted as a function of calcining and reduction temperatures. High reduction and calcining temperatures are detrimental to the sintering of compacts. This is not unexpected as sintering occurs already at about 800°C. The results indicate that optimal sinterability ought to be found at low calcination and reduction temperatures.

2.3 Powder treatment

Treatment to improve sinterability of the powder can be divided into three groups; namely, milling or thermal treatment, sintering promoting additions, and adjustments of the excess oxygen content. Some results from experiments in these three categories have already been published (7). Preliminary results of further tests show that grinding this powder, although it raises the pressed density, does not improve the density of the sintered compact. Pressing difficulties seem to be one reason for this unexpected result.

Additions of SiC and a few alkali halides have not improved sintering.

The role of non-stoichiometric composition in sintering UO_2 has been discussed in several papers (5, 8). Our recent experiments have been limited to powders between $UO_{2.07}$ and $UO_{2.19}$. The influence of the excess oxygen in this range on the sintered density is fairly small. More extensive investigations by Murray and co-workers (9) show that the major effect is to be found below $UO_{2.05}$.

3. COMPACTING PARAMETERS

The effect of cold compacting on sintering has been investigated not only in order to reach a high density but also to study the porosity. Sintering has been conducted in moist hydrogen at 1575°C for 20 hours. Fig. 7 shows the pressed and sintered densities as functions of the specific pressure.

Micro-photographs (fig. 8) indicate that the crystals inside the agglomerates sinter together, while practically no bridges are established between the agglomerates. In sintering pressed compacts, on the other hand, these bridges are formed. The main observation with increasing pressure is that the porosity between the agglomerates is more and more reduced, while the porosity inside them changes very little. The open pores close at about 10,2 g/cm^2 or 93% of theoretical density which is in agreement with Lustman's results (5). The crystal size of the sintered compact increases with increasing specific pressure (9). One rather specific effect of pressure on this particular type of powder is that agglomerates may be broken down into smaller fragments. This generally occurs around 5 ton/cm^2 specific pressure and results in a slightly reduced sintered density, a larger fraction of medium sized pores and reduced crystal size (10). The kinks in the curve in fig. 7 and 9 should not be overlooked. They may very well be caused by this effect.

4. SINTERING VARIABLES

4.1 Temperature and time

In studying the effect of temperature and time on sintering, cold pressed compacts of about 50% theoretical density containing 1, 2% lubricant have been used. Most experiments have been conducted in a molybdenum wound alumina tube furnace, charged with four boats. These where removed after 0, 2, 6 and 20 hours at top temperature. Moist hydrogen, i. e. hydrogen bubbled through room temperature water ($\sim$ 10 g/m^3), was used as atmosphere. The pellets were slowly put into the furnace at 800°C and heated at a rate of 100°C per hour. In fig. 10 the results are plotted so that the whole densification process can be followed. The time zero is defined as the moment the pellet reaches the top temperature. The diagram showing density as a function of temperature (fig. 11) emphasizes the fact that the rate of densification reaches its maximum at a rather low temperature. This has been confirmed by a test series in a high frequency furnace where the temperature could be changed quickly. The temperature program, as well as the results, is shown in fig. 12. The excess oxygen content is removed gradually reaching the stoichiometric composition at about 1500°C (fig. 13). When the run-up is too fast, diffusion zones can be observed as in fig. 14. Both carbon and excess oxygen content are decidedly higher in the central zone.

4.2 Atmosphere

A fairly wide variety of sintering atmospheres has been investigated, generally under the same conditions as mentioned in the preceding paragraph. Steam sintering, however, has been carried out in a molybdenum disilicide furnace. As in many other cases water vapor has a considerable influence on the sintering. A comparison between dry hydrogen, moist hydrogen and steam is given in fig. 15 and 16. The moist hydrogen contained about 10 g/m^3 while the dry hydrogen had a dew point below -60°C entering the furnace. That condition is only valid for the first pellet in the direction of the gas flow. The water vapor formed by reduction of the excess oxygen in the first pellet changes the atmosphere around the following pellets which show higher densities.

Argon has been tested at a few temperatures. In all cases lower densities have been achieved than in dry hydrogen.

Excess oxygen removal is somewhat slowed down by high steam contents while crystal growth is accelerated (fig. 17). In extrapolating to the crystal size of the original powder one gets an idea of the starting temperature for the crystal growth. These temperatures seem to coincide with those where the rate of sintering is highest (fig. 15). If this has any significance is under further investigation.

5. ACKNOWLEDGMENTS

The authors want to express their gratitude to the following persons for their valuable contribution to this work, namely Knut-Erik Jansson, Sven Eriksson, Birgitta Schöning, Harald Björzén, Stig Premfors, Lars Örtenholm, Lars-Göran Bergström and Nils Lundqvist.

6. REFERENCES

1. Margen P. H., Pershagen B.: R3-A Natural Uranium Fuel Heavy Water Moderated Reactor for Combined Electricity Production and District Heating. A/CONF 15/P/135

2. Wivstad I, Mileikowsky C: Adam - a 75 MW nuclear energy plant for house heating purposes. A/CONF 15/P/136

3. Livey D T, Murray P: The technology of UO_2 and ThO_2 Progress in Nuclear Energy, Fuels and Materials.

4. Belle J, Lustman B: Properties of UO_2 US AEC Research and development report WAPD-184

5. Schönberg N, Runfors U, Kiessling R: Production of Uranium Dioxide Bodies for Fuel Elements. A/CONF 15/P/182

6. Gelin R, Mogard H, Nelson B: Refining of Uranium Concentrate and Production of Uranium Oxide and Metal. A/CONF 15/P/179

7. Runfors U: Sintering of UO_2 and different methods to control this procedure. Silicates Industriels, May or June (1958)

8. Vaughan D A, Bridge J R, Allison A G and Schwartz C M: Processing Variables, Reactivity and Sinterability of Uranium Oxides. Industrial and Engineering Chemistry, Oct. (1957) p. 1699.

9. Barnes E, Williams J, Murray P: The science and technology of UO_2 Silicates Industriels, to be published during 1958.

10. Kiessling R, Runfors U: Sintering of UO_2 Symposium Technique sur les Eléments de combustibles. CEA, Paris, Nov. (1957).

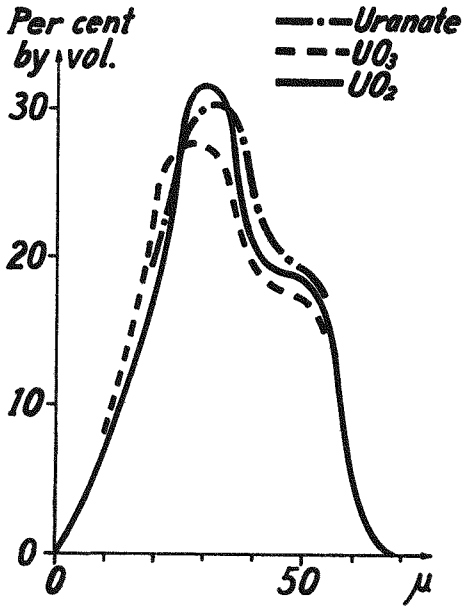

Fig. 1. Agglomerate distribution of an ammonium uranate powder, and the agglomerate distributions of UO_3 and UO_2 subsequently produced from it.

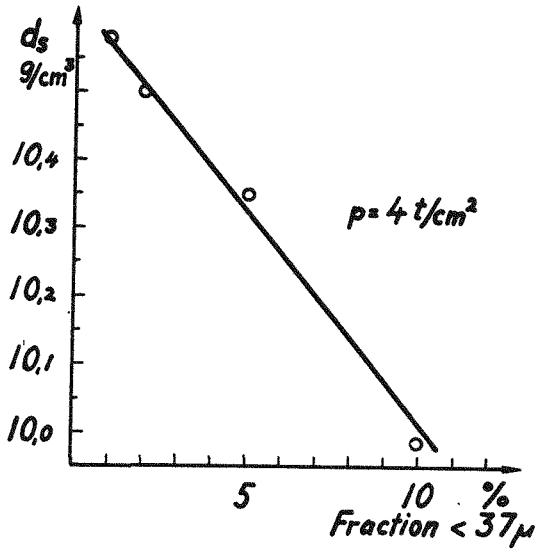

Fig. 2. Sintered density of compacts from four powders as a function of volume-per cent agglomerates below 37 μ.

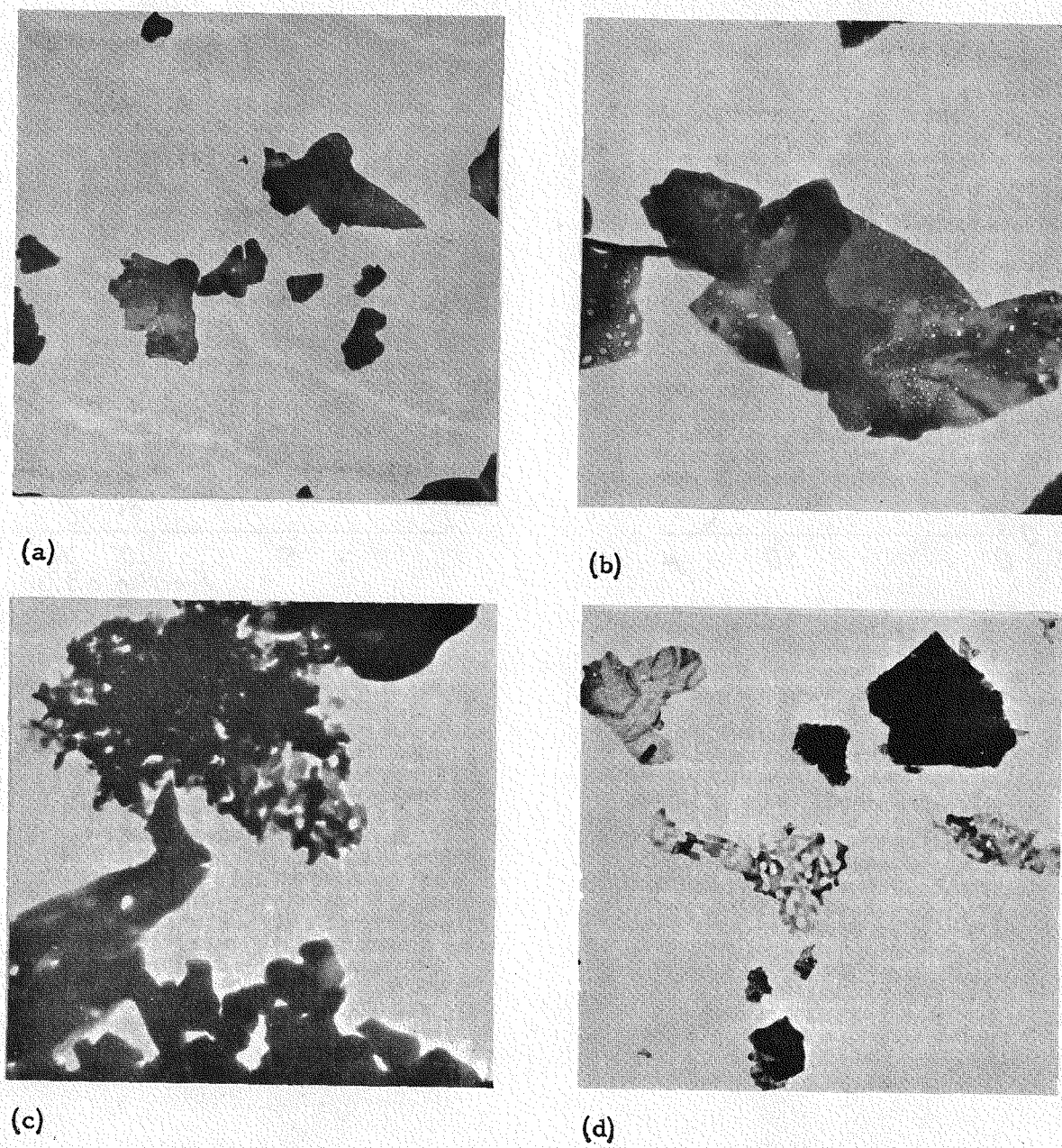

Fig. 3. Crystals of four powders of different sinterability. Compacts of these powders, pressed at 4 t/cm^2, were sintered to the following densities: powder (a) 9,98; powder (b) 10,35; powder (c) 10,50 and powder (d) 10,58 g/cm^3. 34000 x.

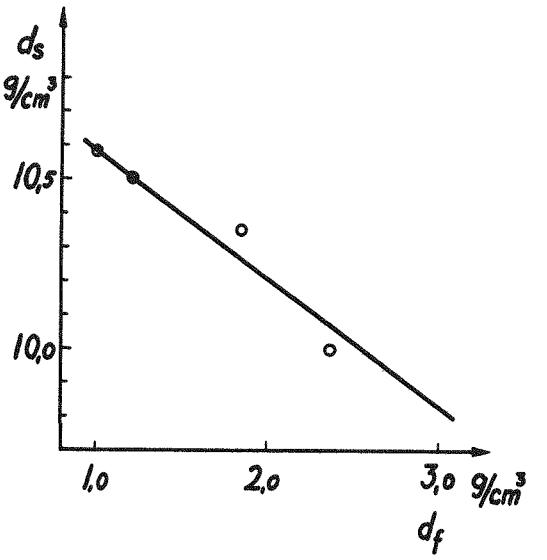

Fig. 4. Density of sintered compacts as a function of bulk density of corres ponding powder

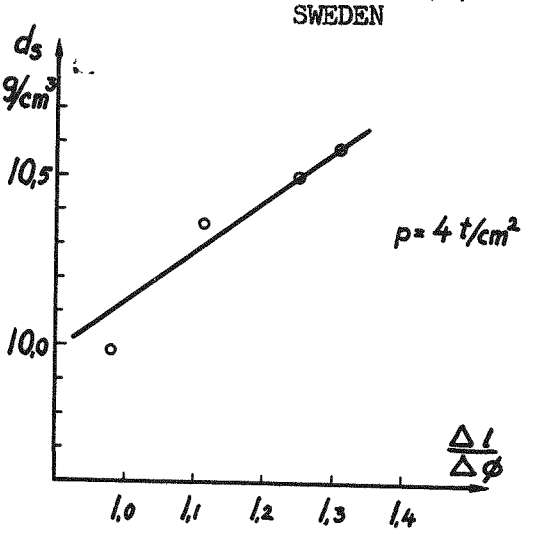

Fig. 5. Density of sintered cylindrical compact as a function of the ratio: shrinkage along the length over shrinkage along the diameter

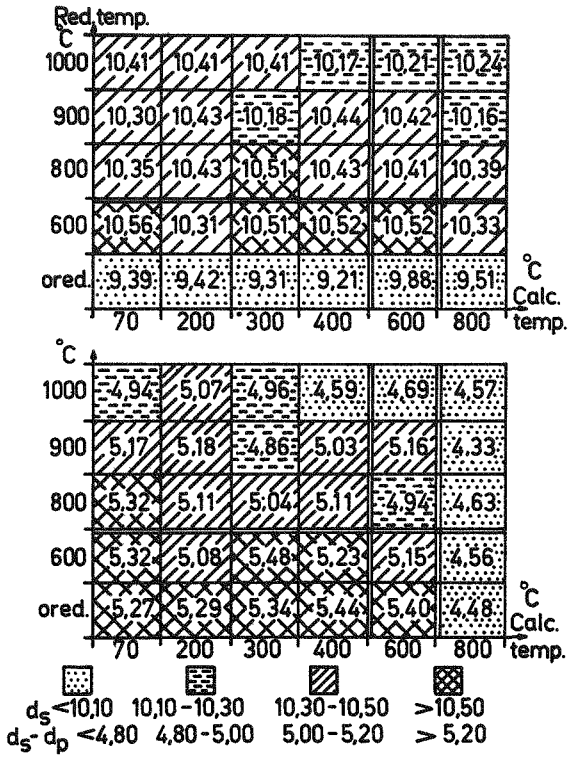

Fig. 6. (above) Density of sintered compacts as a function of calcining and reduction temperatures. (below) Densification (d_s-d_p) as a function of calcining and reduction temperatures.

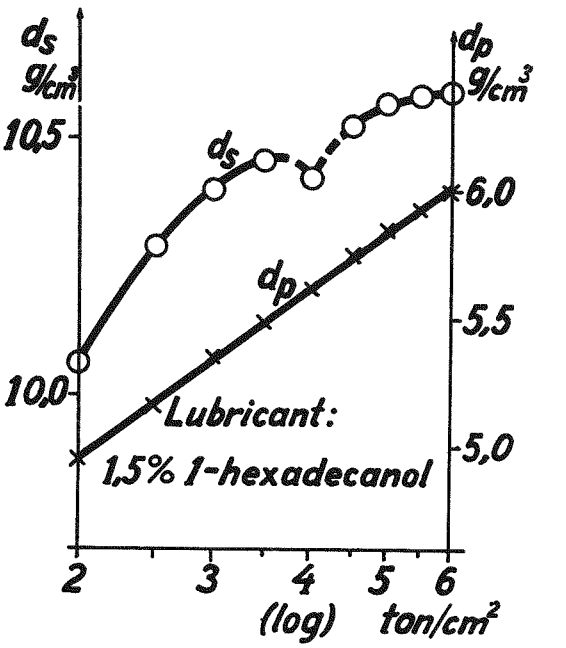

Fig. 7. Pressed and sintered densities of compacts as functions of specific pressure.

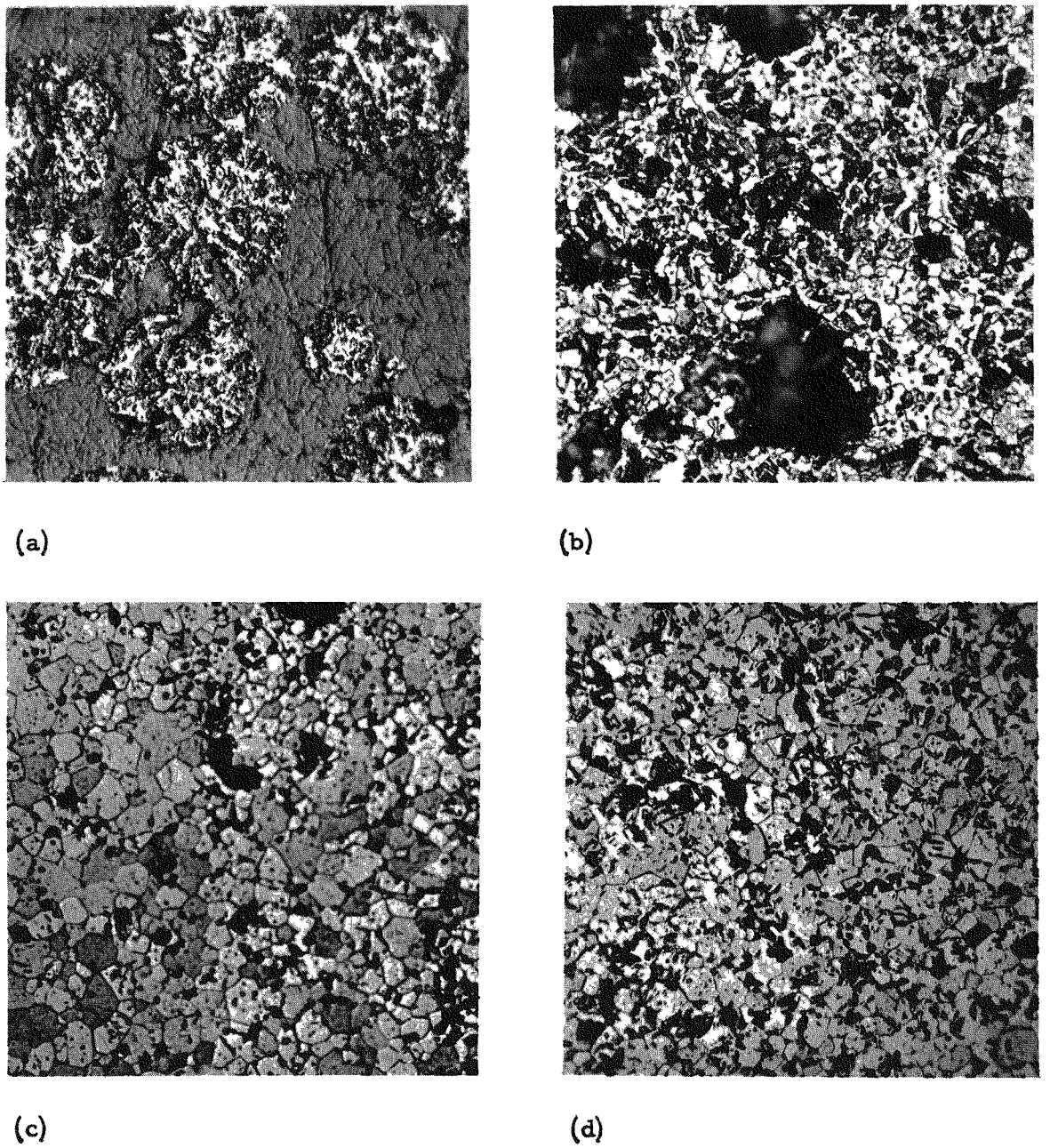

(a) (b)

(c) (d)

Fig. 8. UO_2 agglomerates (sieve fraction 62-74 µ) sintered as loose powder (a), and sintered compacts of the same powder agglomerates pressed at: 0, 75 t/cm^2, 4 t/cm^2 and 5 t/cm^2 (b-d). Gray area between the agglomerates in (a) is plastic matrix. 500 x.

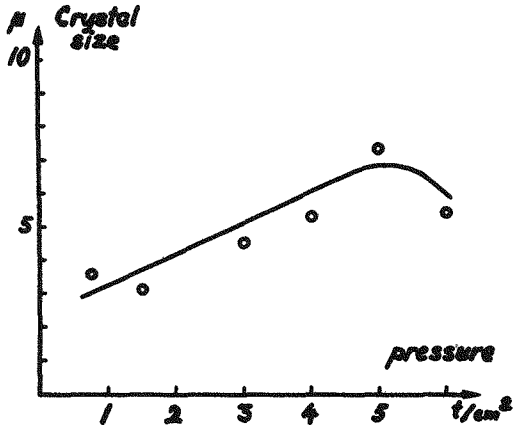

Fig. 9. Crystal size of sintered compacts as a function of specific pressure.

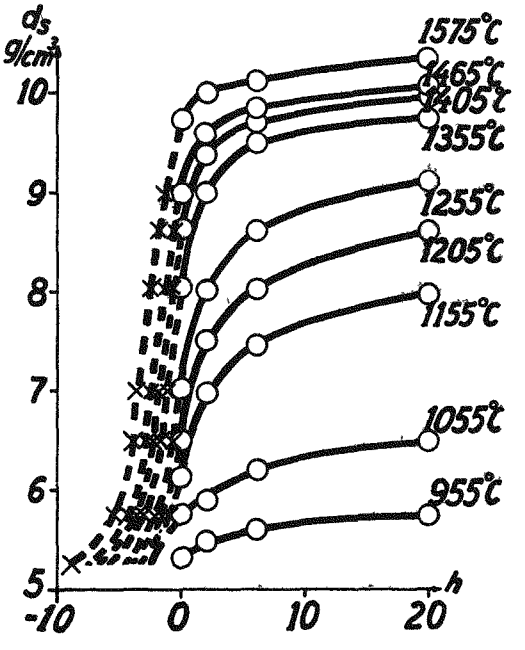

Fig. 10. Sintered density as a function of time at top temperature. Sintering atmosphere: moist hydrogen.

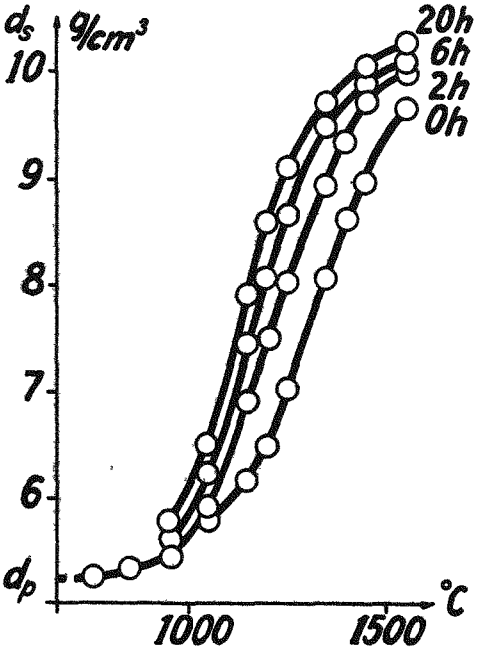

Fig. 11. Sintered density as a function of temperature. Sintering atmosphere: moist hydrogen.

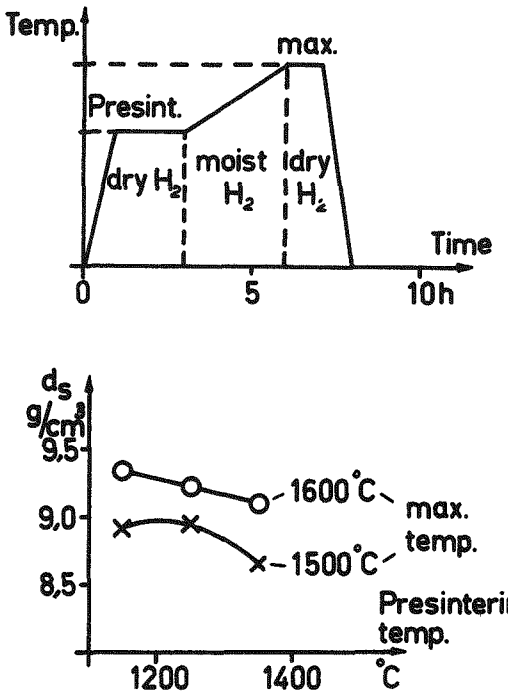

Fig. 12. Sintered density as a function of presintering temperature and top temperature, according to the temperature program shown in diagram above.

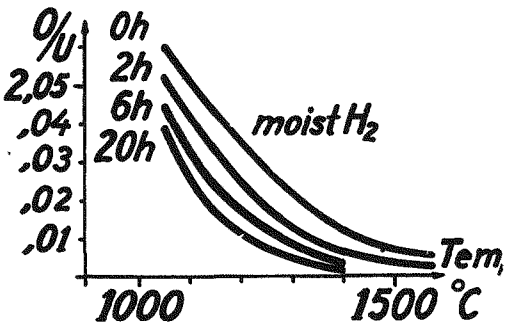

Fig. 13. O/U ratio of sintered UO_2 pellets as a function of temperature and time.

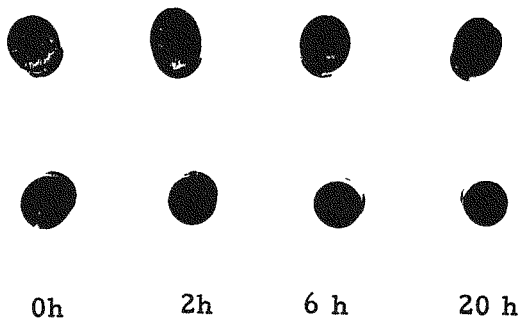

Fig. 14. Diffusion zones in UO_2 pellets sintered at 1185°C (top row) and 1355°C (bottom row) during varying times

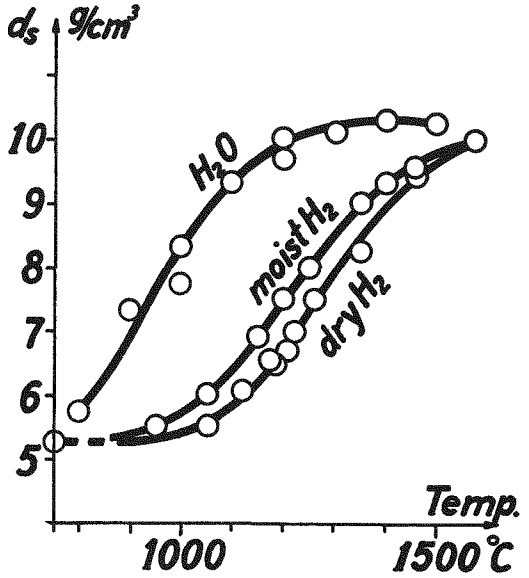

Fig. 15. Comparison between sintered densities obtained in different atmospheres at varying temperatures.

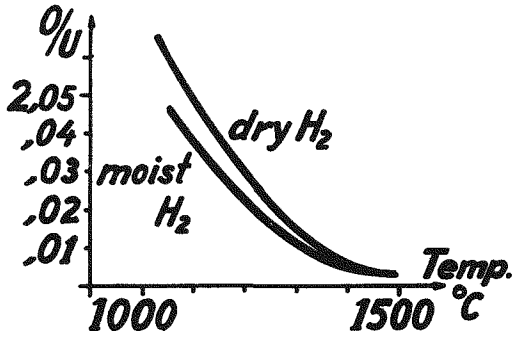

Fig. 16. O/U ratio, of compacts sintered in dry and moist hydrogen for 2 hours, as a function of temperature.

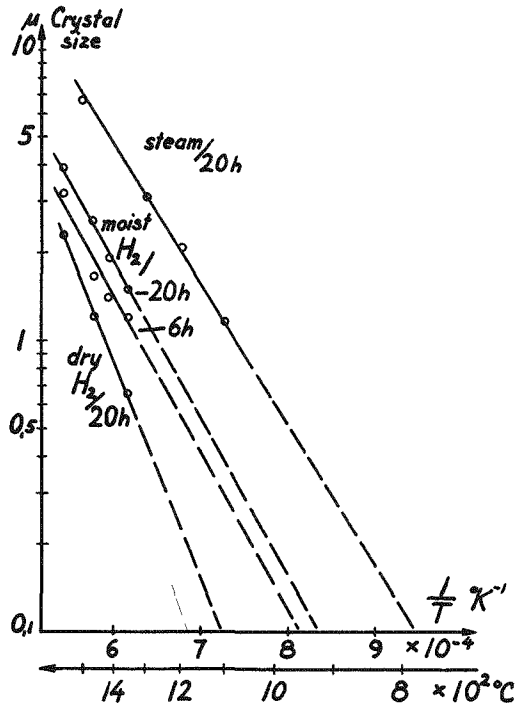

Fig. 17. Log crystal size as a function of inverse sintering temperature.

- - - - -